Supporting Information for

Degradation of *p*-Nitrophenol by Nano-pyrite Catalyzed Fenton Reaction with Enhanced Peroxide Utilization

Tong Liu [1, 2], Nan Chen [2], Yang Deng [2], Fangxin Chen [2], Chuanping Feng [1, 2, *]

[1] MOE Key Laboratory of Groundwater Circulation and Evolution, China University of Geosciences (Beijing), No. 29 Xueyuan Road, Haidian District, Beijing 100083, P.R. China

[2] School of Water Resources and Environment, China University of Geosciences (Beijing), No. 29 Xueyuan Road, Haidian District, Beijing 100083, P.R. China

[*]Corresponding author: Chuanping Feng

Email: *fengcp@cugb.edu.cn*

Phone: (+86)-10-82322281; Fax: (+86)-10-82322281

p-NP analytical method

The concentration of *p*-NP was determined using high-performance liquid chromatography (HPLC 1260, Agilent, US) with a UV-Vis detector. A ZORBAX Eclipse XDB-C18 column (5 μm, 4.6 mm× 250 mm) was used for the separation. A mixture of methanol and water (60/40, v/v) was used as mobile phase. The injection volume was 20 μL, the temperature of the column chamber was set at 30℃, and the detector was operated at 317 nm.

Nano-pyrite characterization

The scanning electron microscopy (SEM, SSX-550, Shimadzu, Japan) was used to characterize the surface morphology of the milled pyrite after gold plating. The X-ray diffraction (XRD) was executed to examine the phase purity and crystal structure of milled pyrite using the XRD analyzer (D8, BRUKER, Germany) with Cu Kα radiation (40 kV, 30 mA). The scan range (2θ) was 20 to 90° with a scan speed of 6°/min. Fourier transform infrared (FT-IR) spectrum was analyzed by the FT-IR analyzer (Nexus 670, Nicolet, US). The X-ray photoelectron spectroscopy (XPS) spectra were obtained with an Escalab 250Xi system (Thermo Scientific, US) with Al Kα radiation at 1486.6 eV for the elemental analysis. The Brunauer-Emmett-Teller (BET) surface area of pyrite was calculated from N_2 adsorption/desorption isotherms using a specific surface area analyzer (Autosorb-IQ2, Quantachrome, US).

GC-MS sample preparation

Two samples (H_2O_2 concentrations of 3 mM and 10 mM) were used to determine the mineralization products of *p*-NP. 30 mL of the nano-pyrite Fenton reaction solution was withdrawn and extracted with 5 mL dichloromethane (GC grade, Sigma Aldrich) for three times. The obtained aqueous solution (using phase separator paper (GE, US)) was concentrated to dryness by nitrogen blowing and then dissolved in 1 mL hexane (GC grade, Sigma Aldrich, dried over anhydrous sodium sulfate) for further analysis.

To determine the high polarity degradation intermediates, N, O-Bis(trimethylsilyl)trifluoroacetamide (BSTFA) was used to produce trimethylsilyl derivatives. The extracted aqueous solution was concentrated to dryness by nitrogen blowing in a 2 mL glass vial. After the addition of 200 μL BSTFA, the vial was closed and stored in an oven at 60℃ for 20 min. Then the vial was added with 1 mL hexane (GC grade, Sigma Aldrich, dried over anhydrous sodium sulfate) for further analysis.

GC-MS analytical methods

For the analysis of intermediates, the samples were analyzed by a GC-MS system (QP2010, Shimadzu, Japan) equipped with an HP5-MS capillary column (0.25 mm 132 i.d. x 30 m with 0.25μm film) using hydrogen as the carrier gas. The injection volume was 1 μL. The injector was set at 280℃, whereas the column was initially set at 50℃ for 5 min, then increased at 5℃/min to 280℃ where it was held for 5 min.

Kinetic fitting

Experimental data obtained in this study can be fitted by pseudo-first-order kinetics.

$$\frac{dC_{p-NP}}{dt} = -k_1 C_{p-NP} \#(S1)$$

In which, $C_{p\text{-NP}}$ referred to the measured *p*-NP concentration, t referred to time, and k_1 was the calculated pseudo-first-order kinetics constant.

To clarify the effects of environmental parameters on *p*-NP degradation kinetics in the heterogeneous Fenton reaction, the experimental data obtained in the early stage were fitted using pseudo-first-order kinetics (Eq. (S1)), and their rate constants were calculated and compared.

***p*-NP mineralization pathway**

The initial degradation step was the electrophilic addition of ·OH onto *p*-NP, leading to the formation of dihydroxycyclohexadienyl radical (DHCHD·). The attack of ·OH

onto *ortho*- and *para*- position of aromatic ring concerning -OH was favored due to mesomeric electron donor effect of the hydroxyl group (-OH), while attack onto *meta*-position concerning nitro-group ($-NO_2$) was preferred because of high electron acceptor effect of $-NO_2$. The electrophilic addition of ·OH onto *ortho*- position leads to the formation of *p*-nitrocatechol, while hydroquinone was produced from the *ipso* attack of ·OH (i.e. the *para*- position of -OH) with $-NO_2$ leave simultaneously. Due to orientation effect of substituents and rapid oxidation of hydroquinone to *p*-benzoquinone [3], *p*-nitrocatechol was foreseen to be the primary hydroxylated derivative of DHCHD·.

Further attack of ·OH on *ortho*- position of hydroquinone and *para*- position (*ipso*) of *p*-nitrocatechol leads to the formation of 1,2,4-trihydroxybenzene. 3,4,5-trihydroxynitrobenzene, which was produced from ·OH attack onto *ortho*- position of *p*-nitrocatechol and was confirmed to be the major product [3], was not detected due to its high polarity and low accumulation.

Due to the strong electrophilic effect of ·OH, the C-C bonds between adjacent -OH are destabilized [3]. Consequently, the oxidative ring-opening reactions are favored at these C-C bonds, leading to the formation of aliphatic compounds. Two of these C-C bonds of 3,4,5-trihydroxynitroenzene can be used for oxidative rupture while 1,2,4-trihydroxybenzene only has one, leading to a faster mineralization of 3,4,5-trihydroxynitroenzene than 1,2,4-trihydroxybenzene, which further explains the low concentration of 3,4,5-trihydroxynitrobenzene in the reaction solution.

Owning to their thermolability, low volatility and high polarity which may affect their analysis using GC-MS [4], carboxylic acids and other hydroxylated organic compounds

were derivatized with BSTFA addition to produce trimethylsilyl derivatives before GC-MS analysis.

The ring-opening of 1,2,4-trihydroxybenzene and pyrogallol produced 3-hydroxymuconic acid and 2-hydroxymuconic acid. C4 carboxylic acids such as succinic acid, maleic acid, and fumaric acid were detected as the consequence of further carbon chain shortening processes [4]. The following reactions between these C4 acids and ·OH lead to the formation of acetic acid, oxalic acid, and formic acid, which were then oxidized to CO_2 and H_2O.

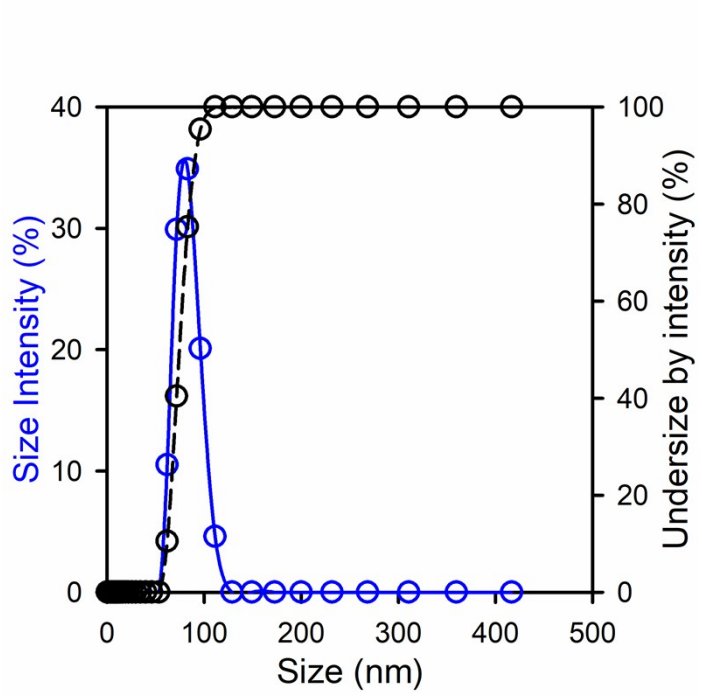

100

101 **Figure S1.** The size distribution of the prepared pyrite nanoparticles dispersed in water.
102 The size measure was carried out with a Malvern laser sizer using disposable sizing
103 cuvette at 4.65 mm height under 25℃ after ultrasonic for 30 min.

104

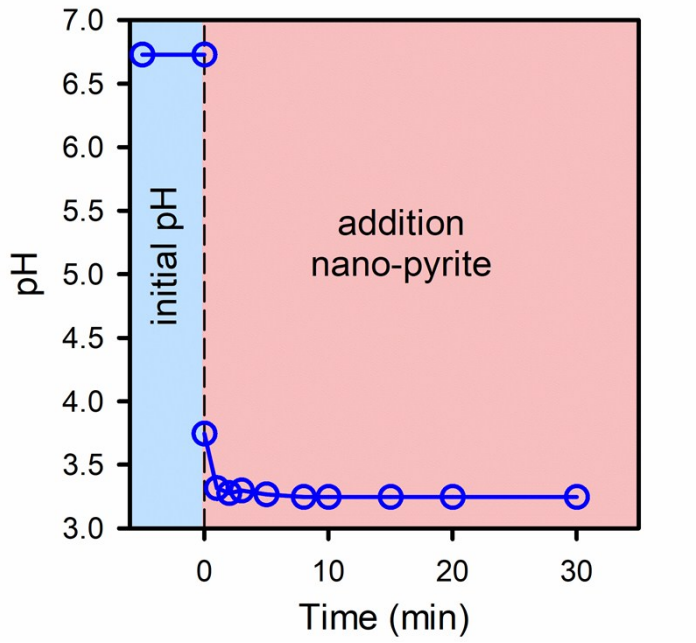

Figure S2. pH variation in nano-pyrite solution. Nano-pyrite dosage = 0.30 g L^{-1}, DIW volume = 100 mL.

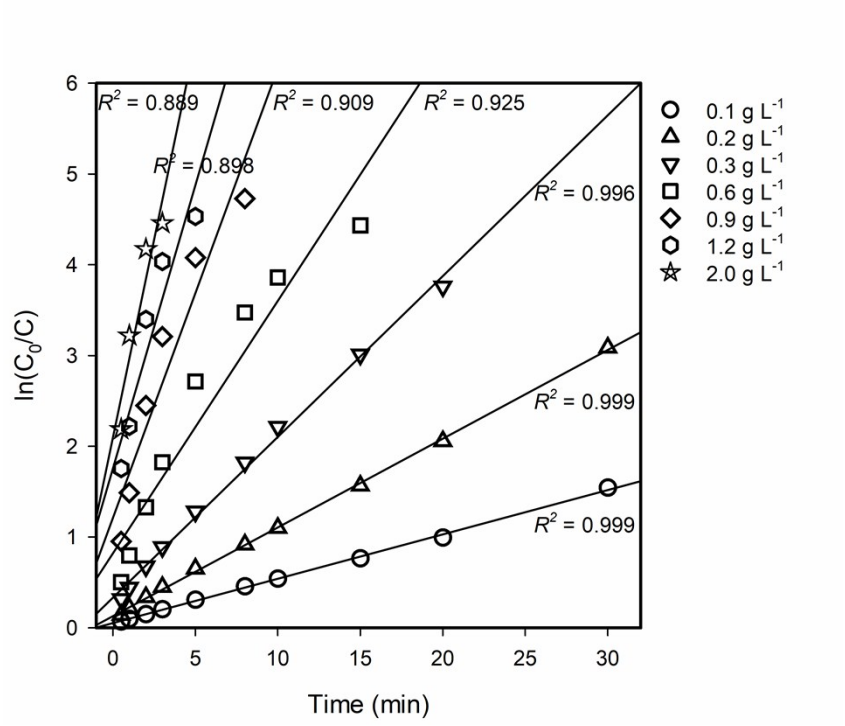

Figure S3. Pseudo-first-order fitting of p-NP degradation kinetics at different nano-pyrite dosages (0.1-2.0 g L^{-1}). Experimental boundary conditions: $[p\text{-NP}]_0$ = 100 mg L^{-1}, initial pH = 4, $[H_2O_2]_0$ = 3 mM, reaction volume = 100 mL, temperature = 25±0.5℃.

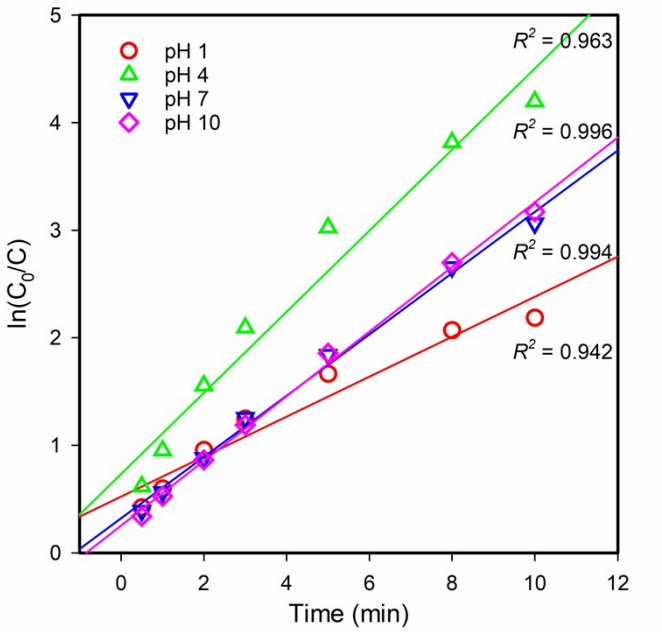

Figure S4. Pseudo-first-order fitting of p-NP degradation kinetics at different initial pH (1-11). Experimental boundary conditions: $[p\text{-}NP]_0$ = 100 mg L-1, nano-pyrite dosage = 0.30 g L^{-1}, $[H_2O_2]_0$ = 3 mM, reaction volume = 100 mL, temperature = 25±0.5℃.

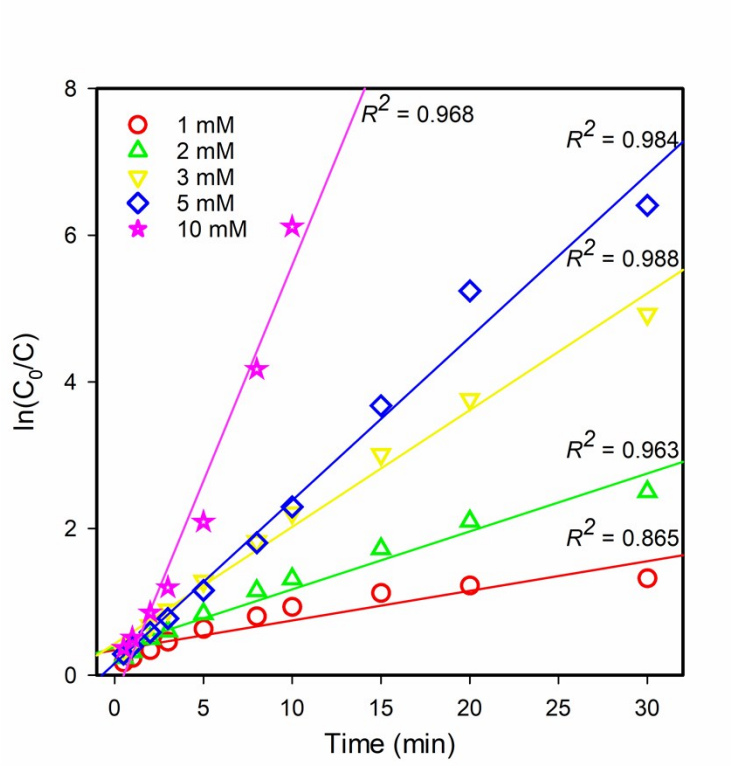

Figure S5. Pseudo-first-order fitting of p-NP degradation kinetics at different H_2O_2 concentrations (1-10 mM). Experimental boundary conditions: $[p\text{-}NP]_0$ = 100 mg L^{-1}, initial pH = 4, nano-pyrite dosage = 0.30 g L^{-1}, reaction volume = 100 mL, temperature = 25±0.5℃.

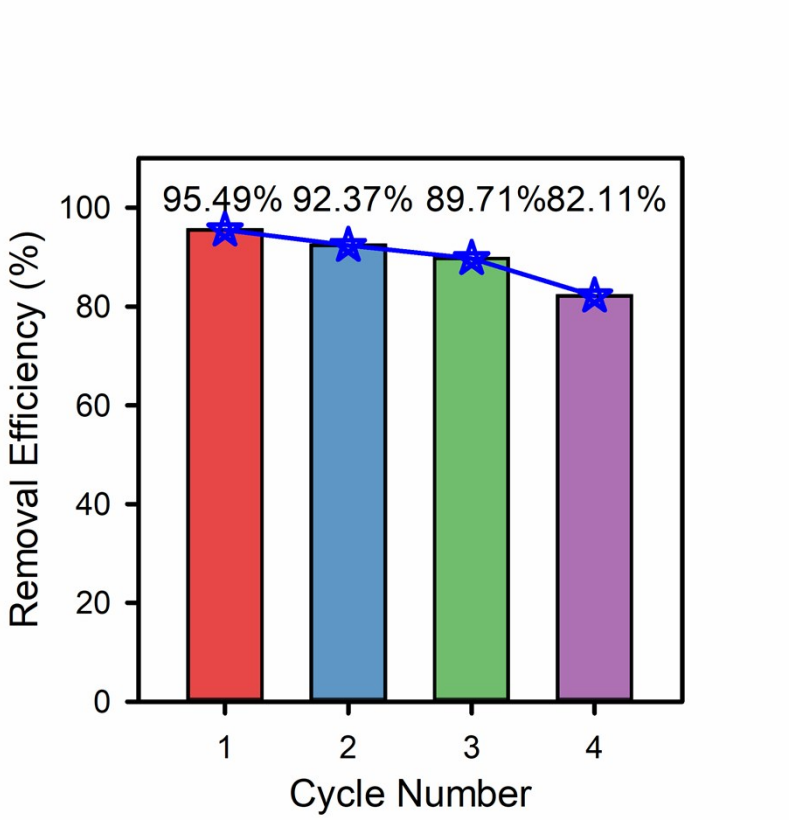

Figure S6. Durability test of nano-pyrite Fenton system and classic Fenton system. 100 mL solution containing 100 mg L^{-1} *p*-NP, 3 mM H_2O_2, and 0.30 g L^{-1} nano-pyrite. *p*-NP and H_2O_2 was added every cycle.

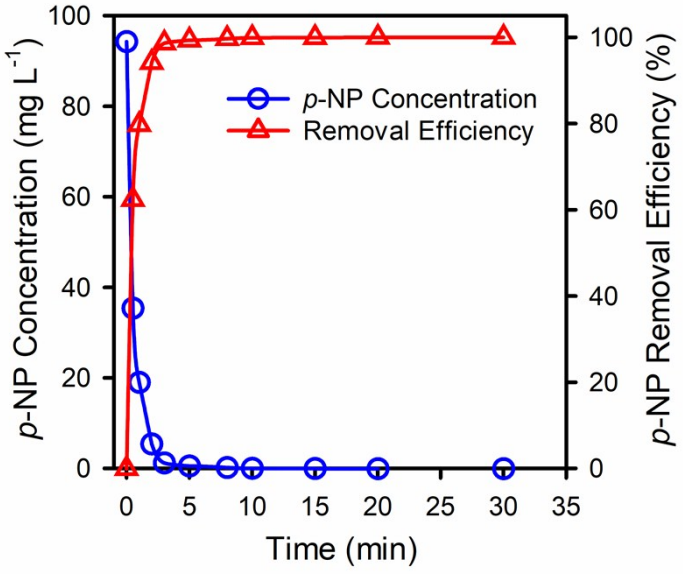

136

137 **Figure S7.** Scale-up experiment for nano-pyrite Fenton system. p-NP degradation by

138 nano-pyrite Fenton system in 1.0 L solution containing 0.30 g L^{-1} nano-pyrite, 100 mg

139 L^{-1} *p*-NP, and 3 mM H_2O_2.

140

Reference

[1]. Bai, Y.; Yeom, J.; Yang, M.; Cha, S.-H.; Sun, K.; Kotov, N. A. Universal Synthesis of Single-Phase Pyrite FeS_2 Nanoparticles, Nanowires, and Nanosheets. *J. Phys. Chem. C* **2013**, *117* (6), 2567–2573.

[2]. Xing, M.; Xu, W.; Dong, C.; Bai, Y.; Zeng, J.; Zhou, Y.; Zhang, J.; Yin, Y. Metal Sulfides as Excellent Co-Catalysts for H_2O_2 Decomposition in Advanced Oxidation Processes. *Chem* **2018**, *4*, 1–14.

[3]. M.A. Oturan, J. Peiroten, P. Chartrin, A.J. Acher, Complete Destruction of p - Nitrophenol in Aqueous Medium by Electro-Fenton Method, Environmental Science & Technology. 34 (2000) 3474–3479. doi:10.1021/es990901b.

[4]. J. Meijide, E. Rosales, M. Pazos, M.A. Sanromán, p-Nitrophenol degradation by electro-Fenton process: Pathway, kinetic model and optimization using central composite design, Chemosphere. 185 (2017) 726–736. doi:10.1016/j.chemosphere.2017.07.067.